The optical activity of carvone: A theoretical and experimental investigation

Cite as: J. Chem. Phys. **136**, 114512 (2012); https://doi.org/10.1063/1.3693270
Submitted: 17 November 2011 . Accepted: 17 February 2012 . Published Online: 20 March 2012

Jason Lambert, R. N. Compton, and T. Daniel Crawford

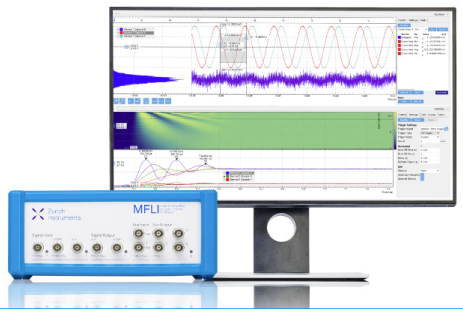

The optical activity of carvone: A theoretical and experimental investigation

Jason Lambert,[1,a)] R. N. Compton,[1,b)] and T. Daniel Crawford[2,c)]
[1]*Department of Physics and Department of Chemistry, University of Tennessee, Knoxville, Tennessee 37996, USA*
[2]*Department of Chemistry, Virginia Tech, Blacksburg, Virginia 24061, USA*

(Received 17 November 2011; accepted 17 February 2012; published online 20 March 2012)

The optical rotatory dispersion (ORD) and circular dichroism of the conformationally flexible carvone molecule has been investigated in 17 solvents and compared with results from calculations for the "free" (gas phase) molecule. The G3 method was used to determine the relative energies of the six conformers. The optical rotation of (*R*)-(−)-carvone at 589 nm was calculated using coupled cluster and density functional methods, including temperature-dependent vibrational corrections. Vibrational corrections are significant and are primarily associated with normal modes involving the stereogenic carbon atom and the carbonyl group, whose $n \rightarrow \pi^*$ excitation plays a significant role in the chiroptical response of carvone. Without the inclusion of vibrational corrections the optical rotation calculated with CCSD and DFT has the opposite sign of experimental data. Calculations of optical rotation performed in solution using the polarizable continuum model were also opposite in sign when compared to that of the experiment. © *2012 American Institute of Physics*. [http://dx.doi.org/10.1063/1.3693270]

I. INTRODUCTION

Solute-solvent interactions are of central importance to chemistry. Numerous studies have focused on the effects of solvents on chemical reactions rates, NMR, UV-Vis, Raman, IR spectroscopy, circular dichroism (CD), and optical rotatory dispersion (ORD). A common approach taken to quantify the effects of solvation is to correlate the properties of solvents (dipole moment, polarizibility, hydrogen bond donation and acceptance, pH, dielectric constant, etc.) with trends in experimental observations.[1] This study focuses on the effects of solvent on the ORD and CD of the carvone molecule and the computational modeling of the ORD and CD of carvone in both the gas phase and in solution.

The carvone molecule shown in Figure 1 is a chiral terpene which exists in two enantiomeric forms, (*S*)-(+)-carvone and (*R*)-(−)-carvone. Both enantiomers are natural products: (*S*)-(+)-carvone is a major component in the oil from caraway seeds and (*R*)-(−)-carvone is present in spearmint oil. As such, both enantiomers are heavily utilized in the food industry. Ballard *et al.*[2] and Suga *et al.*[3] studied the conformational flexibility of carvone using temperature dependent circular dichroism. Ballard *et al.*[2] reported an enthalpy difference of 2.0 kcal/mol between the axial (ax) and the lower energy equatorial (eq) structures of carvone (see Figure 1). The conformational properties of carvone have also been studied using laser jet spectroscopy[4] and gas electron diffraction.[5] Egawa *et al.*[4] determined that the "equatorial 1" conformer was 62% ± 18% abundant at 401 K while the combination of the 2nd and 3rd equatorial conformers were the second most abundant structures. Mineyama *et al.*[5] measured the 1+1 REMPI spectrum of carvone but did not attempt to quantify the abundance of the conformers. It was concluded that the gas phase carvone was primarily composed of the three equatorial conformers distinguished by rotation about the C7−C8 bond shown in Figure 1. Jansík *et al.*[6] studied the conformational flexibility and the magnetochiral birefringence computationally. The populations calculated in their study are similar to the results presented in Table I of this article. The slight differences between this article and their results can likely be ascribed to differences in basis set. The nomenclature for the conformers of carvone used in this article is the same as that used by Egawa *et al.*[4] and Mineyama *et al.*[5]

A large variety of solvent parameters[1,7,8] have been used to quantify the effects of solvation. These include both intrinsic parameters such as solvent dipole moment and empirical parameters such as solvochromatic shifts in the UV/Vis absorption of a chosen reference molecule. The E_T^N values are a normalized unitless empirical parameter calculated using Eq. (1) from the solvochromatic shift of the strongest UV/Vis absorption band of a pyridinium (*N*)-phenolate betaine dye.[1] The reference solvents chosen for the E_T^N values are water and tetramethylsilane (TMS),

$$E_T^N = \frac{\nu_{solvent} - \nu_{TMS}}{\nu_{water} - \nu_{TMS}}. \quad (1)$$

In Eq. (1) $\nu_{solvent}$ is the frequency of the strongest electronic absorption band for the pyridinium dye in the chosen solvent. The Kamlet-Taft parameters characterize a solvent with three parameters α, β, and $\pi^\star$ (Refs. 7 and 1),

$$[\alpha]_\lambda^T = a\alpha + b\beta + c\pi^\star + [\alpha]_{cyclo,\lambda}^T. \quad (2)$$

The term α represents the solvent's propensity toward hydrogen bond donation. The term β represents the tendency of a solvent to accept a hydrogen bond and $\pi^\star$ is a term that accounts for the effects of solvent dipole moment and polarizability. The term $[\alpha]_{cyclo,\lambda}^T$ is the value of the specific rotation

a)Electronic mail: jlamber9@utk.edu.
b)Electronic mail: compton@ion.chem.utk.edu.
c)Electronic mail: crawdad@vt.edu.

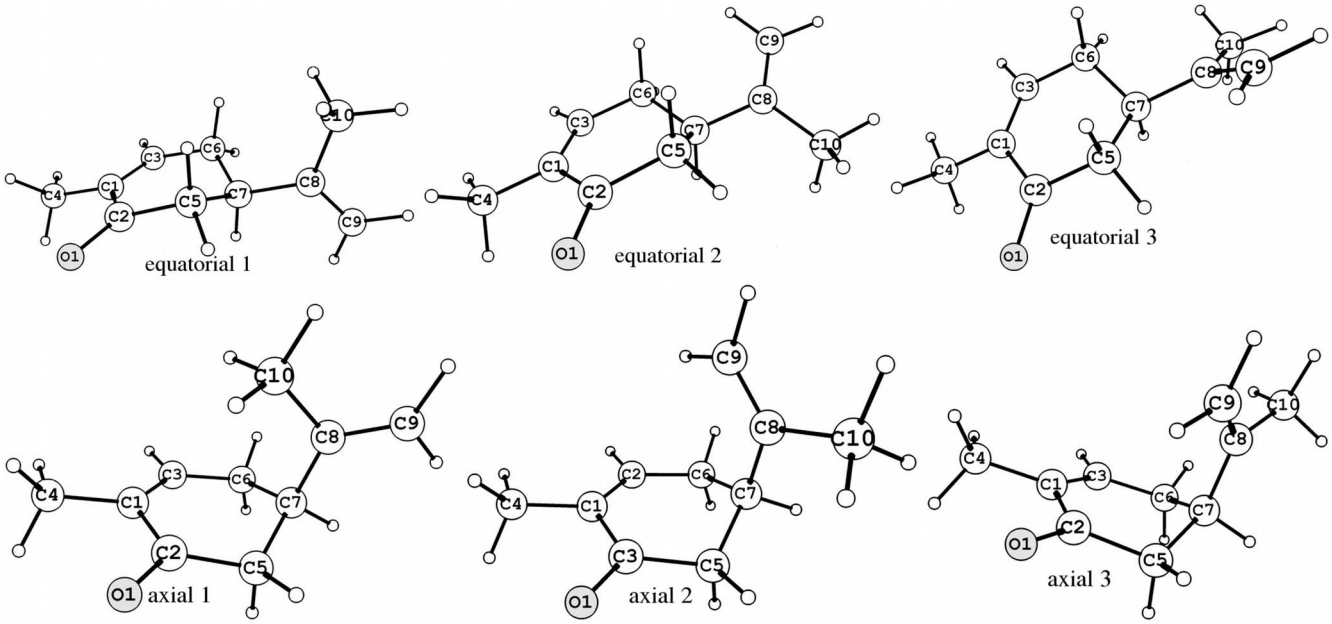

FIG. 1. The six stable conformers of carvone.

at temperature T and wavelength λ in cyclohexane, which is taken to be the least perturbative of the solvents. In Eq. (2), the term a quantifies the hydrogen bond acceptance of the solute. For example, if the solute readily accepts a hydrogen bond then this parameter will be larger in magnitude. The parameter b quantifies the importance of hydrogen bond donation of the solute and the parameter c quantifies the importance of the dipolarity/polarizability term for the solute being studied. The terms a, b, and c are determined through a multivariable linear regression. Once a, b, and c are known for the measured property of the solute, then the value of the solute property being studied can be estimated for all other solvents provided that their Kamlet-Taft parameters are known. The Kamlet-Taft parameters have been applied with mixed success to NMR,[11] UV/Vis,[12] IR,[13] and ORD.[8] The carvone molecule has a hydrogen bond acceptor site, as well, and possesses a dipole moment due to the oxygen double bond attached to the cyclohexane ring. The calculated dipole moment (B3LYP/aug-cc-pVDZ) in the gas phase for each of the three equatorial conformers are 3.6, 3.2, and 3.8 D for the equatorial conformer 1, 2, and 3, respectively (see Figure 1). The Kamlet-Taft parameters are evaluated to determine their applicability to the conformationally flexible carvone molecule.

Quantum chemical calculations have developed rapidly over the past decade but calculations of ORD remain a challenge for electronic structure theory.[14–19] While excellent results have been obtained in most cases when comparing between advanced coupled cluster (CC) methods and gas-phase experimental data,[18,20] agreement with liquid-phase results is much worse.[18,21] Indeed, in some cases, it has been demonstrated that agreement with experiment occurs because of a fortuitous cancellation of errors,[18,22] and calculations of ORD have been known to produce results that differ in sign with that of the experimental data even at high levels of theory. Furthermore, even zero-point vibrational corrections have been found to be important in many cases.[20,23–27] For example, calculations carried out using coupled cluster theory with triples excitations produce the incorrect sign when compared to gas-phase values[28,29] for (*S*)-propylene oxide (methyloxirane),[23] unless vibrational corrections are included as well.[25] The incorporation of such effects, not to mention the additional complexities of conformational flexibility[30–33] and solvation, is a challenging task.

Implicit solvation models are typically based upon the work of Kirkwood,[34] Born,[35] and Onsager,[36] and vary primarily in the manner in which the electrostatic and

TABLE I. Computed relative energies and populations of the conformers of carvone.

	Dihedral angle[a]		Relative energy(kJ/mol)		Populations at 298 K	
Conformer	B3LYP/6-311**	G3	B3LYP/6-311G**	G3	B3LYP/6-311**	G3
1 (eq)	121.7	126.8	0.0	0.0	0.44	0.30
2 (eq)	249.9	251.7	1.3	0.48	0.26	0.25
3 (eq)	348.2	348.3	1.3	0.28	0.26	0.27
1 (ax)	116.2	115.0	8.9	6.4	0.012	0.022
2 (ax)	248.8	241.1	8.7	3.4	0.013	0.075
3 (ax)	355.1	4.8	8.0	3.0	0.017	0.090

[a]Defined as the C9−C8−C7−C5 angle of Figure 1.

non-electrostatic forces are treated and the manner in which the solvent cavity is formed. The electrostatic interactions are the result of the charge distribution of the solute and how it interacts with the polarizable continuum. For example, the molecular dipole can be utilized to polarize the solvent reaction field. Likewise, a multipole expansion of the solute charge distribution centered on an atom or bond can be used similarly. The cavity that forms the solvent exclusion region can be formed by employing simple atomic centered spheres, overlapping van der Waals surfaces, or more complex elliptical shapes. The non-electrostatic forces describe other effects such as the cavitation energy, dispersion forces, and repulsion forces. The polarizable continuum model (PCM) places the solute charge distribution inside an infinite polarizable medium with the dielectric constant ϵ equal to that of the chosen solvent. The solvent reaction field responds to the solute charge distribution and then the solute charge distribution is modified by the solvent reaction field. This model has been successfully applied to a wide variety of problems.[37] However, PCM-based approaches have been useful for ORD computations only in select cases. For example, Mennucci and coworkers[38] combined density functional theory (DFT) calculations of specific rotations with their implicit PCM, and reported sodium D-line rotations in reasonable agreement with corresponding measurements in cyclohexane, acetone, methanol, and acetonitrile, but significant errors appeared for others, such as CCl_4, benzene, and $CHCl_3$. Given the inherent limitations in their model, they attributed the discrepancies to non-electrostatic effects, and role of the functional (B3LYP) in the errors they observed remains unknown. Pecul *et al.*[39] reported analogous DFT-based PCM studies of electronic circular dichroism in 2005 for methyloxirane, camphor, norbornenone, and fenchone. They found that the reliability of their predictions depended not only on the shortcomings of available exchange-correlation functionals but also on the type of transition in question, with Rydberg-type excitations and the $n \rightarrow \pi^*$ transitions of norcamphor and norbornenone were especially problematic, perhaps due to specific solute-solvent interactions.

II. COMPUTATIONAL METHODS

The six stable conformers of carvone shown in Figure 1 were optimized using DFT/B3LYP (Refs. 40–42) with the 6-311G(*d*,*p*) basis set and the higher accuracy G3 method[43] as implemented in GAUSSIAN 03.[44] The G3 and G3MP2 method perform an initial Hartree-Fock/6-31G(*d*) optimization and frequency calculation to determine the zero-point vibrational energy correction. This is followed by a MP2 (full)/6-31(*d*) geometry optimization for both the G3 and the G3MP2 method. Specific rotations for each conformer were computed using linear-response theory in conjunction with the coupled cluster singles and doubles (CCSD) approach,[21,22,45–47] a second-order approximation to CCSD referred to as CC2,[48] and a time-dependent DFT (TD-DFT) formulation[49] with the B3LYP functional.[50] To ensure origin independence of the computed rotations, gauge including atomic orbitals[50–52] were employed with the B3LYP method, and the modified velocity representation of the electric dipole operator was used with the CCSD and CC2 methods.[53] The 1*s* core orbitals for all carbon and oxygen atoms were held frozen in the coupled cluster computations. Optical rotations were computed using the correlation-consistent basis sets of Dunning and coworkers, including one or two sets of diffuse functions as necessary.[54,55] For simplicity, the names of the Dunning basis sets will be abbreviated as follows: DZ = cc-pVDZ, aDZ = aug-cc-pVDZ, aTZ = aug-cc-pVTZ, daDZ= d-aug-cc-pVDZ, aDZ/DZ = aug-cc-pVDZ on carbon and oxygen atoms plus cc-pVDZ on hydrogens, aT(D)Z/DZ = aug-cc-pVTZ on atoms involved in double bonds plus aug-cc-pVDZ on all other carbons plus cc-pVDZ on hydrogens, (d)aDZ/DZ = d-aug-cc-pVDZ on atoms involved in double bonds plus aug-cc-pVDZ all other carbons plus cc-pVDZ on hydrogens. The calculations demonstrate the existence of six stable conformers, in agreement with Harding *et al.* and Jansík *et al.*[6,56] Boltzmann populations were computed using Gibbs free energies from both B3LYP/6-311G(*d*,*p*) and G3 approaches, within the ideal-gas, rigid-rotor, and harmonic-vibration approximations.[57,58] (These populations will be referred to hereafter as "B3LYP" and "G3", respectively.) Contributions from temperature-dependent (300 K) molecular vibrations were computed for each conformer following the approach described by Wiberg *et al.*,[30] using the B3LYP/6-311G(*d*,*p*) harmonic force field. Displacements along each normal mode were computed using stepsizes of 0.05 (cf. Ref. 30). In order to obtain stability of the numerical differentiation, the equilibrium geometries were converged to a root-mean-square force of $1 \times 10^{-6}\ E_h/a_0$, with pruned numerical integration grids of at least 99 radial shells and 509 angular points per shell. All B3LYP computations were carried out using GAUSSIAN 03 (Ref. 44) and GAUSSIAN 09,[59] while all coupled cluster computations were carried out using PSI3.[60]

The PCM model calculations utilized the integral equation formulation using simple united atom topological model to construct the solvent exclusion region as implemented in GAUSSIAN 03.[44] The structure of the six conformers were optimized in each of the solvents listed in Table II using the PCM model coupled with B3LYP/aDZ method and the higher accuracy G3MP2 method.[61] The goal with the usage of the G3MP2 calculations is to obtain more accurate Gibbs free energies which influence the relative populations drastically.

TABLE II. Calculated optical rotation (deg dm^{-1} $(g/ml)^{-1}$) of (*S*)-(+)-carvone using the PCM model. Both the structure and the optical rotation were computed using the aDZ basis set.

	B3LYP/aDZ Wavelength (nm)				
Solvent	436	532	546	578	589
Acetone	−191.1	−71.6	−64.2	−51.2	−47.7
Acetonitrile	−198.0	−76.2	−68.6	−55.0	−51.3
Benzene	−212.6	−80.6	−72.5	−58.2	−54.3
Cyclohexane	−144.3	−29.4	−25.2	−25.2	−18.1
Dimethyl sulfoxide	−200.3	−77.0	−69.4	−55.7	−51.9
Ethanol	−206.3	−81.1	−73.1	−59.0	−55.1
Methanol	−187.8	−70.1	−62.9	−50.1	−46.6
Toluene	−193.6	−73.6	−66.1	−53.0	−49.3

The geometries obtained from optimization with B3LYP/aDZ with the PCM model were used to calculate the optical rotation at 589 nm, 578 nm, 546 nm, and 436 nm. A Boltzmann averaged OR using the Gibbs free energy obtained from B3LYP/aDZ and G3MP2 method was calculated at 25 °C ("G3MP2 Avg"refers to a Boltzmann average in solution using G3MP2 coupled with the PCM model and "B3LYP/aDZ Avg" uses B3LYP/aDZ coupled with the PCM model to calculate Boltzmann averages). As with the gas phase calculations, the populations are determined within the ideal gas, rigid rotor, and harmonic-vibrational approximation with additional corrections for the electrostatic, cavitation, dispersion, and repulsion interactions in solution. All solution phase calculations were performed on (*S*)-(+)-carvone.

III. EXPERIMENTAL METHODS

A. Concentration-dependent ORD

(*R*)-(−)-carvone and (*S*)-(+)-carvone were obtained from Alfa Aesar with a stated purity of 98% and 96%, respectively. These samples of carvone were used for all the experiments in this paper. The quoted specific rotation of the samples were -60.8 deg dm^{-1} (g/ml)$^{-1}$ and 60.2 deg dm^{-1} (g/ml)$^{-1}$. Each solution was prepared without purification using seven or eight different concentrations ranging from 1.28×10^{-3} g/ml to 3.85×10^{-2} g/ml. Data for each wavelength and concentration were measured five times and the average of these five measurements was used to determine the ORD at infinite dilution in order to minimize the effect of solute-solute interactions.[62–64] All the measurements of optical rotation in this article except for the neat value for carvone, are the result of an extrapolation to infinite dilution. Optical rotations were measured at 22 °C to 25 °C using a 10 cm path length at 589 nm, 578 nm, 546 nm, and 436 nm with a Perkin Elmer model 241 polarimeter. With this apparatus the typical fluctuation in the measured angle was 0.002°. The extrapolated intrinsic rotation was determined by fitting the absolute rotation to a fourth-order polynomial, using the constraint that the rotation must decay to zero at zero concentration. The error bars for each measurement are the fitting parameter error bars using a scaled Levenberg-Marquardt algorithm for the fitting. The ORD curves obtained from the extrapolation method were compared to the Drude model to check for consistency. All the fit parameters used in the Drude fitting are given in the supplementary material.[65]

B. Gas and solution phase CD

The solution phase CD was measured using a 1 mm path length in an Aviv Biomedical model 202 CD spectrometer. The gas-phase CD was measured using a 1 cm path length in the same spectrometer with a small amount of sample placed in the bottom of the sample container. Various concentrations were used when preparing the solutions. The temperature of the gas-phase measurements were varied from 20 °C to 60 °C. The gas-phase measurement is unreliable below 250 nm because of the absorption of the quartz cell. The sample container was monitored for condensation on the walls. No obvious condensation was observed but the possibility of a thin layer being deposited on the surface cannot be ruled out, but this should not affect the room temperature data. The data were taken with 4 s of averaging per data point at 0.5 nm steps for both solution and gas phase CD.

IV. RESULTS AND DISCUSSION

A. Experimental ORD

The chemical literature is replete with efforts to correlate properties such as ORD and CD with various properties of solvents, both pure and mixtures. For example, in a series of papers in the 1930s, Rule and coworkers studied the effects of solvent polarity on the specific rotation of several chiral solutes, including, for example, 1-menthyl methyl naphthalate,[66] and found that for solvents of the same type a rough approximation to a smooth curve is obtained when rotatory powers are plotted against dipole moments. However, other studies from the same group found the relationship between the dipole moment of the solvent and the ORD of the solute to be erratic, such as for methylentartaric acid.[67]

In 1970, Kumata *et al.*[68] considered a number of solvent parameters, including dipole moment, Onsager dielectric function,

$$f(\epsilon) = \frac{\epsilon - 1}{2\epsilon + 1}, \tag{3}$$

as well as the $E_T(30)$ parameter, which is defined as the excitation energy corresponding to the maximum absorption of a standard dye in a given solvent.[1] Using propylene oxide (methyloxirane) as a test case, they attempted to correlate such properties with the rotivity, Ω, which is the specific rotation modulated by the Lorentz solvent factor,

$$3\Omega = \frac{3}{n^2 + 2}[\alpha], \tag{4}$$

where n is the index of refraction of the solvent. While they did find reasonable correlation between Ω and solvent polarity, the relationship with other parameters was considered "poor," apart from indicating "a general trend."

More recently, Wiberg *et al.*[69] studied the ORD of (*S*)-2-chloropropionitrile in different solvents, and compared their measured rotations to the corresponding Onsager reaction field values. While most solvents exhibited reasonable correlation between the two, the measured rotation in benzene fell far below that of the other solvents, and the extrapolated ($\epsilon = 1$) gas-phase value of -21 deg dm^{-1} (g/ml)$^{-1}$ was nearly a factor of three smaller than that measured via cavity ring-down polarimetry at -8 deg dm^{-1} (g/ml)$^{-1}$. In 2006, Fischer *et al.*[8] correlated the extrapolated ORD of 3-methylbenzylamine with the various solvent parameters and the Kamlet-Taft parameters. 3-methylbenzylamine was chosen because it both donates and accepts hydrogen bonds. There was no strong correlation for any of the chosen solvent parameters in their study, and they reported an R^2 value of 0.667 when comparing experimental data to Kamlet-Taft parameters.

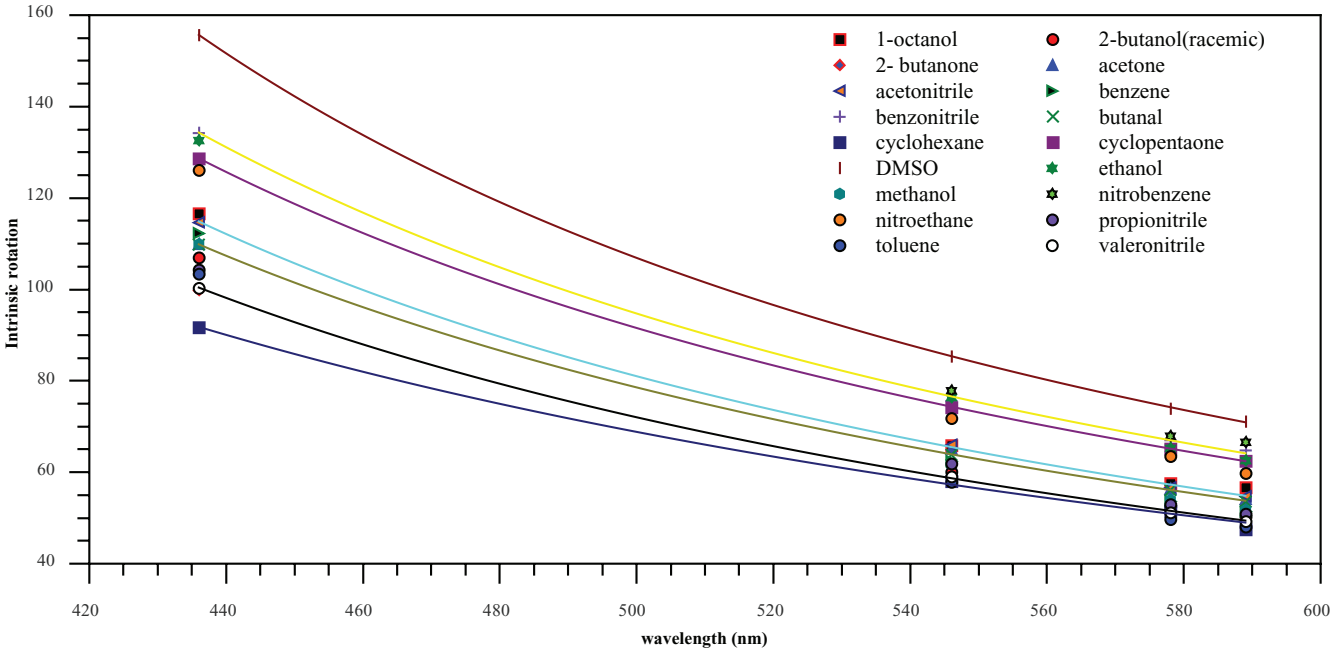

FIG. 2. The ORD of S-(+)-carvone in 17 different solvents fit to a one parameter Drude model. For clarity some of the Drude model fits have been omitted but the parameters for those fits are included in the supplementary material.[65]

Measurements of the ORD for (*S*)-(+)-carvone dissolved in 17 different solvents are summarized in Table III, and the ORD is seen to fit well with the Drude model as shown in Figure 2, regardless of solvent. This fitting opens the question as to what solvent characteristics have the most significant influence on the rotation. Thus, using the values of the ORD at 589 nm, linear fits were made to the solvent parameters of Table IV. The resulting correlation was generally weak, and the strongest match ($R^2 = 0.611$) was obtained with the dipolarity/polarizability Kamlet-Taft parameter, π^*. The solvent dipole moment and dielectric constant had correlation values of $R^2 = 0.442$ and $R^2 = 0.455$ while other terms did not have a significant correlation. A least-squares fit of Eq. (2) was then carried out using the measured value of the specific rotation in cyclohexane ($[\alpha]^T_{0,\lambda} = 44.69$ deg dm^{-1} (g/ml)$^{-1}$) as a constraint, yielding values of a, b, and c of -9.16, 11.04, and 9.83, respectively, and an average root-mean-squared difference between the experimental and calculated ORD of 4.1 deg dm^{-1} (g/ml)$^{-1}$. The slope of the best fit line and its R^2 value are 0.98 and 0.95 in Figure 3 is close to the ideal slope of 1. This fit leads to the tenuous conclusion that the ORD of carvone most strongly depends upon the dipolarity/polarizability of the solvent and that hydrogen bonding has little effect. This does not agree with the expectation that the terms a and c should be larger in magnitude. However, the overall correlation between the experimental data and the Kamlet-Taft parameters remains relatively weak (see Figure 3), suggesting that other factors—conformer populations, molecule-specific solvent-solute interactions, etc.—must be considered for a more complete understanding.

TABLE III. Measured ORD of (*S*)-(+)-carvone (deg dm^{-1} (g/ml)$^{-1}$).

Solvent	436	546	578	589
1-octanol	116.7 ± 11.1	66.0 ± 5.8	57.6 ± 5.0	56.8 ± 4.8
2-butanol (racemic)	107.0 ± 13.9	60.1 ± 7.9	52.6 ± 6.8	50.4 ± 6.4
2-butanone	100.9 ± 5.3	59.0 ± 3.3	52.0 ± 3.0	49.8 ± 2.8
Acetone	110.0 ± 5.1	65.2 ± 2.8	56.4 ± 2.8	54.2 ± 2.6
Acetonitrile	114.8 ± 9.4	66.2 ± 5.3	56.8 ± 4.8	54.8 ± 4.8
Benzene	112.4 ± 13.6	62.5 ± 7.9	53.8 ± 7.4	51.6 ± 7.0
Benzonitrile	134.4 ± 7.0	75.7 ± 3.8	67.1 ± 3.4	64.9 ± 2.8
Butanal	109.9 ± 8.6	64.0 ± 5.0	56.2 ± 4.7	53.7 ± 4.1
Cyclohexane	91.7 ± 7.9	58.1 ± 5.9	51.6 ± 4.4	47.6 ± 5.8
Cyclopentanone	128.7 ± 8.9	74.3 ± 5.3	65.2 ± 4.4	62.5 ± 4.6
Dimethyl sulfoxide	155.7 ± 12.1	85.4 ± 6.7	74.0 ± 5.4	71.1 ± 5.3
Ethanol	132.7 ± 14.3	76.5 ± 8.5	65.3 ± 7.3	62.7 ± 6.8
Methanol	110.0 ± 4.4	61.8 ± 2.8	54.1 ± 2.6	51.8 ± 2.7
Nitrobenzene	None	77.9 ± 3.3	68.0 ± 2.6	66.7 ± 2.7
Nitroethane	126.2 ± 15.6	71.9 ± 9.1	63.5 ± 8.1	59.8 ± 8.0
Propionitrile	104.4 ± 1.7	61.9 ± 1.4	53.0 ± 1.5	51.0 ± 1.5
Toluene	103.4 ± 8.5	57.9 ± 4.7	49.7 ± 4.1	48.1 ± 3.9
Valeronitrile	100.4 ± 6.2	59.1 ± 3.7	51.3 ± 3.0	49.3 ± 3.0
Neat	...	...	...	61.0

B. Experimental gas-phase and solution-phase CD spectra

Measured UV-visible and CD spectra for (*R*)-(−)-carvone dissolved in cyclohexane are shown in Figure 4. We note that the positive CD vibrational features correlate exactly with the vibrational peaks in the UV-visible spectrum in the $n \rightarrow \pi^\star$ transition, but, most interestingly, the negative CD peaks do not correlate with their UV-visible counterparts. CD spectra of carvone in 11 different solvents are shown in Figure 5, and the sign, width, and positions of the peaks are observed to vary with the choice of solvent. For the ketone solvents, the CD is noisy at short wavelength because of strong solvent absorption. Also, for benzene and

TABLE IV. Solvent parameters used in this study (Refs. 1, 8, and 9).

Solvent	E_T^N	ϵ	n(D)[a]	μ(Debye)	α	β	π^*
1-octanol	0.54	10.30	1.43	2.00	0.77	0.81	0.40
2-butanol	0.51	16.56	1.40	1.65	0.69	0.80	0.40
2-butanone	0.33	18.11	1.38	2.78	0.06	0.48	0.67
Acetone	0.35	20.56	1.36	2.88	0.08	0.48	0.62
Acetonitrile	0.46	35.94	1.34	3.44	0.19	0.40	0.66
Benzene	0.11	2.27 (Ref. 10)	1.50 (Ref. 10)	0.00	0.00	0.10	0.55
Benzonitrile	0.33	25.20	1.53	4.28	0.00	0.37	0.88
Butanal	NA	NA	1.38	3.22	0.00	0.40	0.65
Cyclohexane	0.01	2.02	1.43	0.00	0.00	0.00	0.00
Cyclopentanone	0.27	14.45[b]	1.44	3.28	0.00	0.52	0.76
Dimethyl sulfoxide	0.44	46.45	1.48	4.10	0.00	0.76	1.00
Ethanol	0.65	24.55	1.36	1.65	0.86	0.75	0.54
Methanol	0.76	32.66	1.33	2.88	0.98	0.66	0.60
Nitrobenzene	0.32	34.78	1.56	4.22	0.00	0.39	1.01
Nitroethane	0.40	28.96	1.39	3.65	0.00	0.25	0.80
Propionitrile	0.40	28.26	1.37	4.00	0.00	0.37	0.64
Toluene	0.10	2.38 (Ref. 10)	1.49	0.30	0.00	0.11	0.49
Valeronitrile	0.36	20.03	1.40	4.12	0.00	na	0.63

[a]Index of refraction at the sodium D line.
[b]Measured at 20 °C.

valeronitrile, the CD was above the maximum measurable of 0.5° of ellipticity at 320 nm. It is interesting to note that the relative intensity and sign of vibronic peaks change with choice of solvent around 355 nm. Each of the six conformers will interact with each solvent differently. Therefore, the solvent environment is expected to affect both the conformer populations as well as the rotational strengths of each for different transitions.

The solution phase CD in Figures 5 and 4 spectra show significant shifting and even sign changes for particular vibronic peaks in the $n \rightarrow \pi^*$ transition region from 300 to 400 nm. The structure seen in the $n \rightarrow \pi^\star$ transition between 400 and 300 nm has been reported previously by Ballard *et al.*[2] who attributed them to vibrational structure due primarily to the carbonyl stretching mode at $\nu \simeq 1200\ \mathrm{cm}^{-1}$. Our analysis does not support this interpretation because the

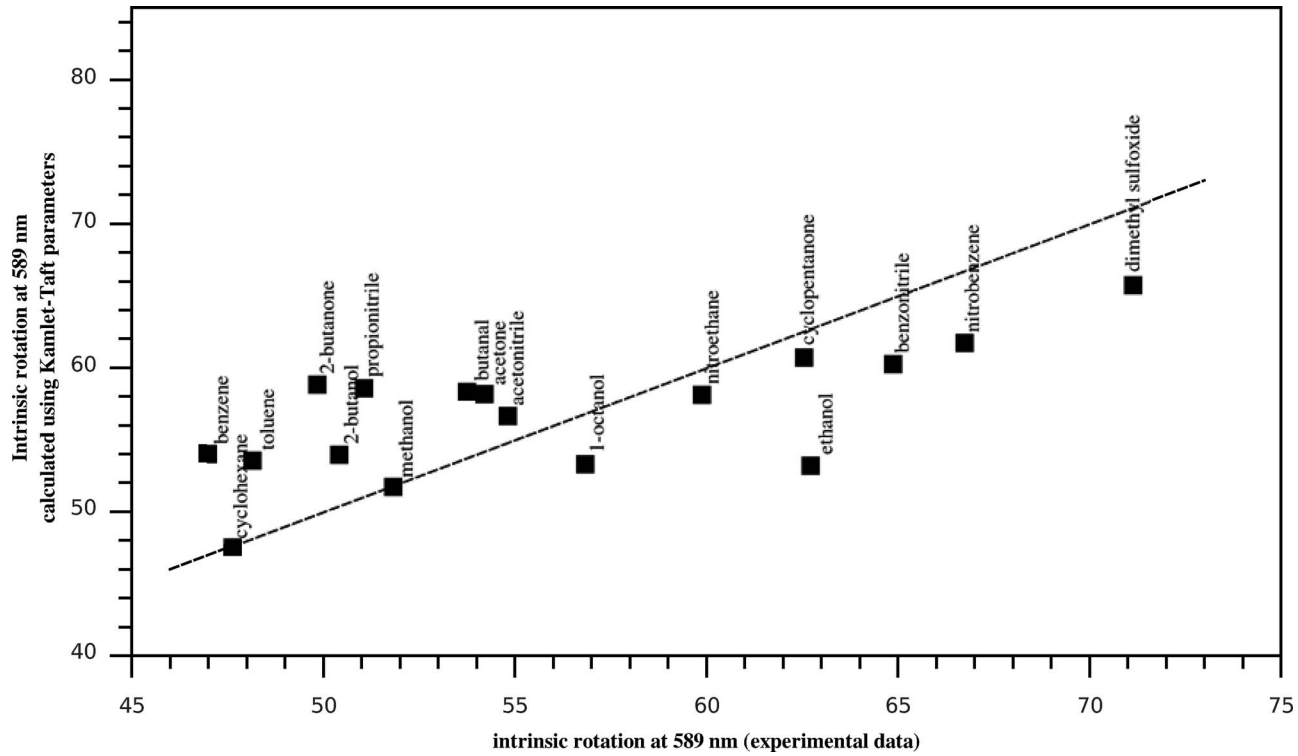

FIG. 3. Plot of data calculated using the Kamlet-Taft parameters found in this study versus the measured experimental optical rotation at 589 nm. The line represents perfect correlation between the experimental and calculated values.

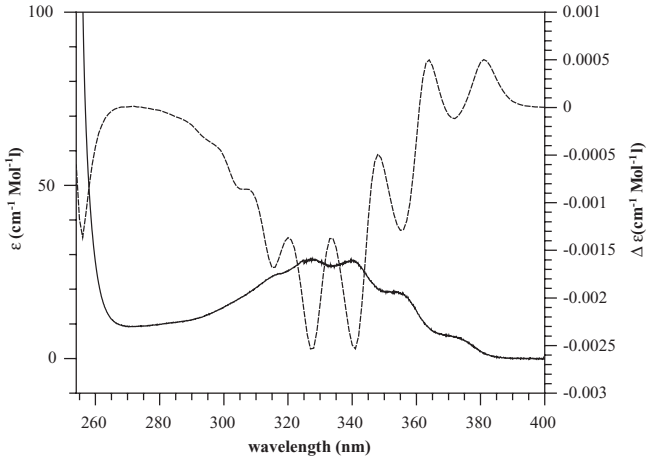

FIG. 4. Representative CD (dashed line) and UV/visible (solid line) spectrum of (*S*)-carvone in cyclohexane.

frequency for the carbonyl stretching mode was calculated to be greater than 1700 cm^{-1} when using B3LYP with both aDZ and 6-311G(*d*,*p*) basis sets. Instead, the vibrational states from 971 cm^{-1} to 1226 cm^{-1} involving ring deformations, propene bending, C−C stretching, and hydrogen bending and rocking are the bands making the largest contribution to the CD in the $n \rightarrow \pi^{\star}$ region. The $n \rightarrow \pi^{\star}$ peaks given in Table V have spacings of $\simeq$1000 cm^{-1}. It is also interesting to note the redshifting of the onset of the peak located at $\simeq$266 nm as the temperature increases. This could be a peak broadening effect from the increased pressure or it is also possible that this is the result of more specific gas-phase molecular interactions similar to the Franck-Condon solvation principle.

Similar vibrational structure is seen in the gas-phase electronic circular dichroism (ECD) spectrum shown for comparison in Figure 6. It is particularly interesting to note that the ECD for carvone in strongly polar molecules such as acetonitrile resembles that for the gas phase or in cyclohexane (cf. Figure 4). This is reminiscent of the observation by Vaccaro and coworkers[29] that their gas-phase ORD measurements

TABLE V. Transition energies of the $n \rightarrow \pi^{*}$ peaks and corresponding energy differences between adjacent peaks in the (*R*)-carvone ECD spectrum.

Wavelength (nm)	E (cm^{-1})	ΔE (cm^{-1})
373.5	26 773.76	0.00
360.0	27 777.78	1004.02
348.0	28 735.63	957.85
335.0	29 850.75	1115.11
322.5	31 007.75	1157.01
311.5	32 102.73	1094.98

more closely resemble those measured in polar rather than non-polar solvents. We propose a possible explanation for the non-perturbing nature of certain highly polar molecules on the ORD and ECD of certain chiral molecules. Molecules with dipole moments greater than 2.5 D are known to form very diffuse, weakly bound dipole-bound anions.[70–74] The extra electron exists in a very diffuse orbital at an extended distance from the molecular framework. Klahn *et al.*[75] and Mikulski *et al.*[76] have measured the mobility of excess electrons in CH_3CN (dipole moment = 3.925 D) and HCN (dipole moment = 2.985 D) and found a strong gas density dependence of the "zero-field" density-normalized mobility (μn). Both CH_3CN (Ref. 70) and HCN (Ref. 77) are known to form dipole bound anions. In order to rationalize this anomalous effect, they proposed a transport process in which short-lived dipole-bound anions (lifetime $\geq$ 12 ps) as quasilocalized states are produced and electrons "hop" from one dipole to another. It is possible that a similar situation can exist in solution in which the excited electron in the excitation of carvone enters into a dipole-bound quasi-stationary state of the polar solvent. The excess electron is proposed to rapidly "jump" from one surrounding dipole to the next with little scattering effects. Thus, the solvent provides a type of "band structure" which only slightly perturbs the excited electron through scattering.

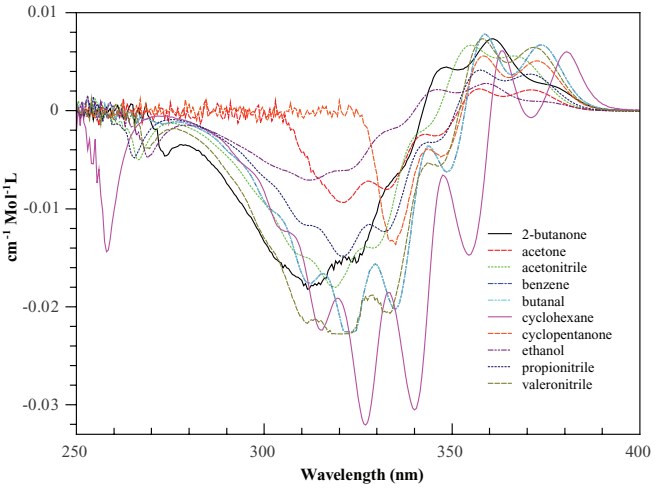

FIG. 5. CD spectra of (*S*)-(+)-carvone in various solvents. The acetone and cyclopentanone data sets have large error below 315 nm and 340 nm, respectively, due to solvent absorption.

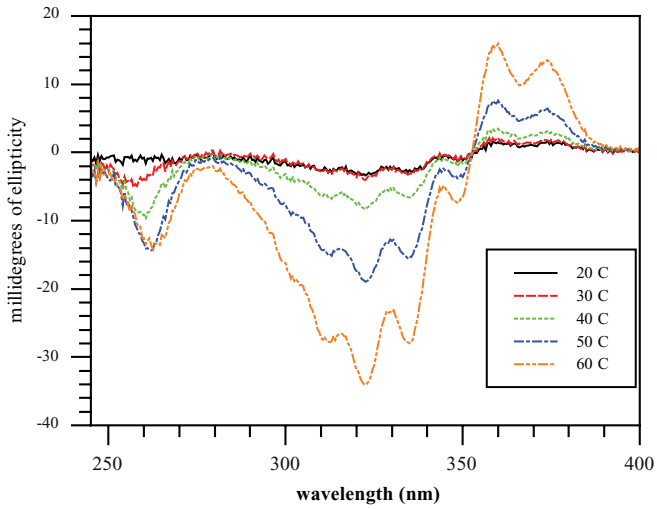

FIG. 6. Measured gas phase ECD of (*S*)-(+)-carvone in millidegrees of ellipticity.

TABLE VI. Specific rotations (in deg dm^{-1} (g/ml)$^{-1}$) of (*R*)-(−)-carvone at 589 nm computed using B3LYP and various basis sets with ($\langle[\alpha]_D\rangle$) and without ($[\alpha]_D$) vibrational corrections from Table IX.

	B3LYP					
	aDZ		daDZ		aTZ	
Conformer	$[\alpha]_D$	$\langle[\alpha]_D\rangle$	$[\alpha]_D$	$\langle[\alpha]_D\rangle$	$[\alpha]_D$	$\langle[\alpha]_D\rangle$
1 (eq)	191.2	109.1	195.6	113.5	193.2	111.1
2 (eq)	237.4	381.1	240.3	384.0	242.2	385.9
3 (eq)	− 340.1	− 458.8	− 341.1	− 459.8	− 336.8	− 455.5
1 (ax)	− 66.4	− 166.5	− 73.2	− 173.3	− 66.3	− 166.4
2 (ax)	82.4	106.4	81.1	105.03	82.2	106.1
3 (ax)	− 230.1	− 377.4	− 231.7	− 379.1	− 225.9	− 373.2
B3LYP[a]	53.8	20.5	56.1	22.7	56.8	23.5
G3[b]	8.8	− 25.8	10.1	− 24.4	11.8	− 22.8

[a]Boltzmann average over conformer rotations using the B3LYP/6-311G(*d*,*p*) populations of Table I.
[b]Boltzmann average over conformer rotations using the G3 populations of Table I.

TABLE VIII. Specific rotation (in deg dm^{-1} (g/ml)$^{-1}$) of (*R*)- carvone at 589 nm computed using CCSD and the aDZ/DZ basis set with ($\langle[\alpha]_D\rangle$) and without ($[\alpha]_D$) vibrational corrections from Table IX.

	CCSD	
Conformer	$[\alpha]_D$	$\langle[\alpha]_D\rangle$
1 (eq)	112.7	30.6
2 (eq)	201.4	345.2
3 (eq)	− 231.0	− 349.7
1 (ax)	− 59.4	− 159.5
2 (ax)	7.6	31.6
3 (ax)	− 183.5	− 330.8
B3LYP[a]	38.1	4.7
G3[b]	4.4	− 30.2

[a]Boltzmann average over conformer rotations using the B3LYP/6-311G(*d*,*p*) populations of Table I.
[b]Boltzmann average over conformer rotations using the G3 populations of Table I.

C. Theoretical calculations of ORD

Table I summarizes the relative energies and corresponding Boltzmann populations at 298 K for each of the six relevant conformers of carvone in the gas phase. Initial computations using the B3LYP/6-311G(*d*,*p*) method indicated that the three axial conformers have energies at 8.0 kJ/mol and higher relative to the lowest-energy conformer and thus contribute no more than 1.7% to the average specific rotation at room temperature. However, subsequent computations using both DFT and coupled cluster methods employing only the equatorial conformers yielded specific rotations at 589 nm for (*R*)-(−)-carvone ranging from 20 to 63 deg dm^{-1} (g/ml)$^{-1}$, i.e., qualitatively incorrect results compared to experiment (cf. Table III for the (*S*) enantiomer). Higher level conformer computations using the G3 method produced significantly different energetics, with the three equatorial conformers much closer in energy and two of the axial conformers falling to within 3.4 kJ/mol of the lowest-energy equatorial structure. The corresponding populations at 298 K indicate that the axial conformer cannot be neglected as together they contribute more than 18% of the total average.

Tables VI–VIII report specific rotations at 589 nm for all six conformers with various basis sets at the B3LYP, CC2, and CCSD levels of theory, respectively. All three methods agree that the individual conformers exhibit substantially different specific rotations, much larger than the absolute value of that measured in solution. (See Table III.) Two of the three lower-energy equatorial conformers give positive rotations for the (*R*) enantiomer (which has a negative rotation experimentally). On the other hand, two of the three axial conformers exhibit negative rotations—another reason that their contribution must be included for accurate computations. The basis-set dependence of the B3LYP results is small; only a few deg dm^{-1} (g/ml)$^{-1}$ shift between the aDZ, daDZ, and aTZ basis sets is observed. The basis-set dependence of the CC2 method is somewhat larger, but the use of a triple-zeta basis on the doubly bonded atoms (aT(D)Z/DZ) tends to produce the opposite shift from the use of extra diffuse functions on the same atoms [(d)aDZ/DZ]. Only one basis set (aDZ/DZ) was possible with the more expensive CCSD method, but some estimate of the impact of higher angular momentum and diffuse

TABLE VII. Specific rotations (in deg dm^{-1} (g/ml)$^{-1}$) at 589 nm computed using CC2 and various basis sets with ($\langle[\alpha]_D\rangle$) and without ($[\alpha]_D$) vibrational corrections from Table IX.

	CC2							
	aDZ/DZ		aDZ		aT(D)Z/DZ		(d)aDZ/DZ	
Conformers	$[\alpha]_D$	$\langle[\alpha]_D\rangle$	$[\alpha]_D$	$\langle[\alpha]_D\rangle$	$[\alpha]_D$	$\langle[\alpha]_D\rangle$	$[\alpha]_D$	$\langle[\alpha]_D\rangle$
1 (eq)	94.6	12.5	99.9	17.9	107.6	25.5	99.9	17.8
2 (eq)	203.9	347.6	203.9	347.6	221.9	365.6	203.6	347.3
3 (eq)	− 291.6	− 410.3	− 292.5	− 411.2	− 297.1	− 415.8	− 288.4	− 407.1
1 (ax)	− 97.4	− 197.5	− 95.3	− 195.4	− 110.4	− 210.5	− 98.9	− 199.0
2 (ax)	11.7	35.6	22.1	46.1	7.8	31.8	14.2	38.2
3 (ax)	− 212.6	− 360.0	− 214.4	− 361.7	− 221.6	− 368.9	− 212.6	− 359.9
B3LYP[a]	14.1	− 19.2	16.4	− 17.0	22.7	− 10.7	17.2	− 16.1
G3[b]	− 19.8	− 54.4	− 17.8	− 52.3	− 14.4	− 48.9	− 17.3	− 51.8

[a]Boltzmann average over conformer rotations using the B3LYP/6-311G(*d*,*p*) populations of Table I.
[b]Boltzmann average over conformer rotations using the G3 populations of Table I.

functions can be obtained by comparison with the CC2 data. While diffuse functions are requisite, including such functions on the hydrogen atoms makes little difference in this case. For example, at the CC2 level of theory using the aug-cc-pVDZ basis set on the carbon and oxygen atoms but only cc-pVDZ on the hydrogen atoms yields an optical rotation at 589 nm of 94.6 deg dm^{-1} (g/ml)$^{-1}$, while extending the hydrogen atom basis set to aug-cc-pVDZ given a rotation of 99.9 deg dm^{-1} (g/ml)$^{-1}$. Two Boltzmann averages are reported in Tables VI–VIII, *viz.* those from the B3LYP/6-311G(*d*,*p*) structures and those from the G3 computations, with the latter expected to be significantly more accurate for a gas-phase simulation. For every method, the G3 populations yield a more negative average rotation for the (*R*) enantiomer, because G3 gives greater weight to the equatorial 3 and axial 3 conformers both of which have strong negative rotations. However, for the B3LYP and CCSD methods, the G3 populations still do not produce overall negative specific rotations for (*R*)-(−)-carvone, in disagreement with experiment. At the B3LYP level, the aTZ basis set gives a G3-averaged rotation of 11.8 deg dm^{-1} (g/ml)$^{-1}$, and at the CCSD level, the aDZ/DZ basis set gives a corresponding 4.4 deg dm^{-1} (g/ml)$^{-1}$. The CC2 method, however, does give negative rotations (with all basis sets used here) when the G3 populations are employed. The CC2/(d)aDZ/DZ level gives an average rotation of −17.3 deg dm^{-1} (g/ml)$^{-1}$. (Note that the B3LYP populations produce the incorrect sign for all methods.)

Given previous findings that vibrational contributions to ORD can be significant in some cases,[20,23–27] we also computed harmonic vibrational corrections for each conformer of (*R*)-carvone. The corrections were obtained at 298 K using numerical differentiation of B3LYP/aDZ specific rotations along the normal modes computed at the B3LYP/6-311G(*d*,*p*) level of theory and are summarized in Table IX. Most striking is the overall magnitude of the correction compared to the equilibrium value. For the equatorial 1 conformer, for example, the total correction is −82.1 deg dm^{-1} (g/ml)$^{-1}$, as compared to a B3LYP/aDZ equilbrium rotation of +191.2 deg dm^{-1} (g/ml)$^{-1}$. In this case, the largest contributions to the vibrational correction arise from three vibrational modes: the twist of the propylene group attached to the stereogenic carbon at C7 (42.3 cm^{-1}, a shift of −89 deg dm^{-1} (g/ml)$^{-1}$), a ring-rocking mode involving the same carbon (105.1 cm^{-1}, −38 deg dm^{-1} (g/ml)$^{-1}$), and the carbonyl stretching vibration (1751 cm^{-1}, +20 deg dm^{-1} (g/ml)$^{-1}$). These and similar vibrations dominate the overall corrections for all six conformations, which is not surprising, given the importance of both the stereogenic carbon and the carbonyl $n \rightarrow \pi^*$ excitation to the chiroptical response of carvone.

Application of the vibrational corrections given in Table IX to the equilibrium rotations shifts the Boltzmann averaged results closer to experiment for all methods. The vibrationally averaged rotations are also given in Tables VI–VIII. For the B3LYP method, the best result is approximately −24 deg dm^{-1} (g/ml)$^{-1}$ (B3LYP/daDZ), while for CC2 and CCSD the best vibrationally averaged results are ca. −52 and −30 deg dm^{-1} (g/ml)$^{-1}$, respectively, which bracket the value of $[\alpha]_D$ measured in cyclohexane (see Table III) of −44.7 deg dm^{-1} (g/ml)$^{-1}$(corrected for the choice of enantiomer). Greater accuracy would be obtained from inclusion of anharmonicities as well as the use of CC-based vibrational corrections. We note that the B3LYP and CCSD averages are reasonably close to one another, even though the specific rotations of the individual conformers differ dramatically in some cases. The tendency of B3LYP to overestimate the specific rotation is related to its concomitant tendencies to underestimate excitation energies[22,26] and to overestimate CD rotational strengths.[25]

The theoretical ORD in each solvent listed in Tables II and X was calculated using the Gibbs free energy obtained using B3LYP/aDZ and the G3MP2 method coupled with the PCM model. There are two significant differences between the Boltzmann populations obtained in each solvent using B3LYP/aDZ and G3MP2 energies. The solution phase B3LYP/aDZ Avg is dominated by the eq(1) conformer in all solvents while the G3MP2 avg has a more equitable distribution of population between the equatorial conformers. In ethanol the B3LYP/aDZ population of eq(1) conformer is 46% of the total populations compared to a G3MP2 Avg population of 32%. In fact, for the aromatic solvents benzene and toluene, the eq(2) conformer is the most stable structure followed by the eq(1) and eq(3) structures. The axial conformers make an insignificant contribution to the total ORD with the B3LYP/aDZ Avg. For example, in ethanol the axial conformers make up 4% of the total population and contribute 3.5 deg dm^{-1} (g/ml)$^{-1}$ to a total specific rotation of −58.6 deg dm^{-1} (g/ml)$^{-1}$. With the G3MP2 Avg the axial conformers make up 17% of the total population and

TABLE IX. Harmonic vibrational corrections (in deg dm^{-1} (g/ml)$^{-1}$) to the specific rotation at 589 nm for each conformer of (*R*)-carvone.

B3LYP/aDZ//B3LYP/6-311G(*d*,*p*)	
Conformer	Vibrational Correction
1 (eq)	− 82.1
2 (eq)	143.7
3 (eq)	− 118.7
1 (ax)	− 100.1
2 (ax)	24.0
3 (ax)	− 147.3

TABLE X. Calculated optical rotation (deg dm^{-1} (g/ml)$^{-1}$) of (*S*)-(+)-carvone using the PCM model. The ORD was calculated using structures optimized with B3LYP/aDZ and the relative population of each conformer was determined using the Gibbs free energy obtained from G3MP2 calculations.

	G3MP2 Wavelength (nm)				
Solvent	436	532	546	578	589
Acetone	− 104.8	− 34.3	− 30.3	− 23.3	− 21.4
Acetonitrile	− 60.6	− 9.3	− 6.9	− 3.1	− 2.1
Benzene	− 116.2	− 41.8	− 37.3	− 29.5	− 27.4
Cyclohexane	− 45.5	− 1.0	0.7	3.4	4.0
Dimethyl sulfoxide	− 62.1	− 16.2	− 13.4	− 8.7	− 7.5
Ethanol	− 75.2	− 18.3	− 15.4	− 10.5	− 9.2
Methanol	− 41.7	− 0.3	1.4	3.9	4.4
Toluene	− 87.3	− 22.7	− 19.3	− 13.7	− 12.3

contribute 20 deg dm^{-1} $(g/ml)^{-1}$ to the total rotation versus the equatorial contribution of −29 deg dm^{-1} $(g/ml)^{-1}$. The ORD at five wavelengths is summarized in Tables II and X. In all cases the use of the G3MP2 Avg pushed the results closer to the experimentally measured positive rotation. In the case of methanol and toluene the rotation was calculated to be positive for four of the five wavelengths. However, the calculated ORD does not have the correct form because it becomes more negative as the wavelength decreases. Additional corrections are needed to obtain a qualitatively correct ORD in solution. Based upon the gas phase results, it is likely that the vibrational corrections need to be considered to bring a solvent phase calculations into agreement with experimental results.

D. Theoretical calculations of ECD

The electronic circular dichroism of (*S*)-(+)-carvone was calculated using TD-DFT/B3LYP with the aDZ basis set without the inclusion of corrections due to excited state geometry changes, Franck-Condon factors, and vibronic coupling between the ground and excited states.[78,79] The calculated rotational strengths and oscillator strengths for 10 transitions of all the conformers are given in the supplementary material.[65] The CD plotted in Figure 7 was calculated using the following equations:

$$CD_i = 0.0247 \sum_{j=1}^{N} \frac{R_j \nu_j}{\sigma} e^{\frac{(\nu-\nu_j)^2}{\sigma^2}}, \tag{5}$$

$$CD_{total} = \sum_{1}^{6} P_i \cdot CD_i, \tag{6}$$

where CD_i is the CD for the ith conformer, R_j is the rotational strength 10^{-40} erg esu cm Gauss^{-1}, ν_j is the frequency in cm^{-1}, respectively, of each CD band, and P_i is the population of the ith conformer. The peak broadening parameter σ was chosen to be 2000 cm^{-1}.[80] The positions of the excited states are close to expected values based upon the CD spectrum and data from Mineyama *et al.*[5] The measured excited state transition at 266.72 nm for the equatorial 1 conformer is close to the calculated value of 265 nm.[5] There is not significant agreement between theory and experiment because of the lack of vibrational structure in the ECD. The calculated position of the $n \rightarrow \pi^\star$ for this ketone is 349 nm which is in the correct range of experimental data. The frequencies of the calculated transitions was scaled by a factor of 0.95, so the wavelength matched the highest intensity peak of the ECD in the $n \rightarrow \pi^\star$ region. The position of the electronic features were close to their expected positions, but the lack of vibrational contributions is believed to be the primary explanation for the large disagreement between experimental and theoretical ECD for the $n \rightarrow \pi^\star$ transition. Any correction to obtain an accurate CD spectrum would need to include vibronic coupling into the theory. The circular dichroism for carvone in the gas phase and in solution with various solvents including cyclohexane have the same general structure. The structure of the ECD over the $n \rightarrow \pi^\star$ in the gas phase and in each solvent starts negative and crosses zero to become positive but the position of the zero crossing, the number of peaks to the left and right of the zero crossing varies and the resolution changes with solvent choice. Nonetheless, it is unlikely that the difference in sign of theoretical and experimental ORD is due to solvent effects. Based upon the calculations in Figure 7 there should be many other strong ECD features below 250 nm.

V. SUMMARY AND CONCLUSIONS

We have carried out both experimental and theoretical studies of the optical activity of carvone in order to elucidate the potential importance of solvent effects on its ORD and CD spectrum. Correlation of the experimentally determined ORD in various solvents with a variety of parameters, including dipole moments, Kamlet-Taft parameters and others, suggest that solvent polarization plays the most significant role in the measured response. However, the correlation in this case is still weak, which is not surprising given that such parameters do not take into account the conformational flexibility of the carvone solute. Experimental CD measurements confirm the vibrational structure in the $n \rightarrow \pi^*$ regime reported earlier, though the previous assignment of this progression to the

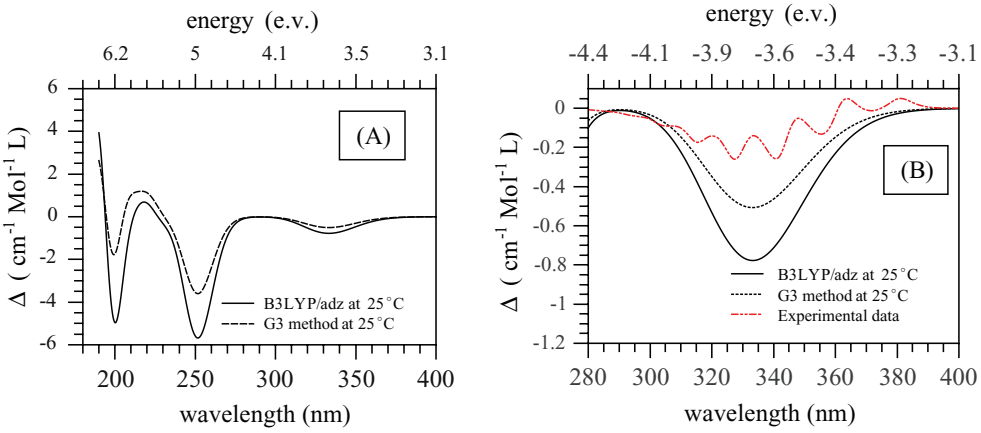

FIG. 7. Computed ECD spectrum of (*S*)-(+)-carvone. (A) Plot of theoretical ECD calculated using populations from the G3 method and B3LYP/aDZ. (B) Comparison of theory and experimental CD of (*S*)-(+)-carvone in cyclohexane.

carbonyl stretching mode is not borne out by quantum chemical computations. Interestingly, the gas-phase CD spectrum agrees better with solution-phase CD spectrum taken in polar rather than non-polar solvents. We offer a hypothesis for this phenomenon based on the observation that solvents with strong dipole moments (>2.5 D) can exhibit a "band" structure in which electrons (such as those excited from the solute) can occupy quasi-stationary states of the solvent molecules. Such a band structure will not exist for non-polar solvents, which thus perturb the solute's diffuse excited states more strongly compared to the gas-phase. Although this hypothesis is appealing and appears to account for the current set of observations, more experimental and computational studies will be necessary to test it.

High-level coupled cluster computations of the ORD of carvone are found to yield incorrect signs compared to solution-phase experiments unless accurate Boltzmann populations and harmonic vibrational corrections are included. While some of the discrepancy between theory and experiment in this case undoubtedly arises from the lack of incorporation of solvent effects in the former, in this case it appears to be more important to model the conformer energetics correctly and to include temperature-dependent vibrational motion. Also, the inclusion of solvent effects using the PCM model predicts results similar to the gas-phase calculations when the same method and basis set are used and vibrational corrections are not included. This further supports the argument that vibrational corrections are of primary importance to calculating an accurate ORD in the case of carvone.

ACKNOWLEDGMENTS

This work was supported by grants from the U.S. National Science Foundation. Contributions from the University of Tennessee were funded by Grant No. CHE-0650524, and those from Virginia Tech by Grant No. CHE-1058420 and a Multi-User Chemistry Research Instrumentation and Facility (CRIF:MU) award CHE-0741927. Also the authors would like to thank undergraduate student Jin Shim for his assistance in recording some of the experimental measurements of ORD.

[1]C. Reichardt, *Solvents and Solvent Effects in Organic Chemistry*, 3rd ed. (Wiley, 2003).
[2]R. E. Ballard, S. F. Mason, and G. W. Vane, Discuss. Faraday Soc. **35**, 43 (1963).
[3]T. Suga and K. Imamura, Bull. Chem. Soc. Jpn. **45**, 2060 (1972).
[4]T. Egawa, Y. Kachi, T. Takeshima, H. Takeuchi, and S. Konaka, J. Mol. Struct. **658**, 241 (2003).
[5]M. Mineyama and T. Egawa, J. Mol. Struct. **734**, 61 (2005).
[6]B. Jansík, A. Rizzo, L. Frediani, K. Ruud, and S. Coriani, J. Chem. Phys. **125**, 234105 (2006).
[7]R. W. Taft, J.-L. M. Abboud, and M. J. Kamlet, J. Am. Chem. Soc. **103**, 1080 (1981).
[8]A. T. Fischer, R. N. Compton, and R. M. Pagni, J. Phys. Chem. A **110**, 7067 (2006); Y. Marcus, *The Properties of Solvents* (Wiley, 1998).
[9]M. J. Kamlet, J. L.M. Abboud, M. H. Abraham, and R. W. Taft, J. Org. Chem. **48**, 2877 (1983).
[10]S. Lata, K. Singh, and S. Ahlawat, J. Mol. Liq. **147**, 191 (2009).
[11]M. J. Kamlet and R. W. Taft, J. Am. Chem. Soc. **98**, 377 (1976).
[12]M. J. Kamlet, M. E. Jones, R. W. Taft, and J. Abboud, J. Chem. Soc., Perkin Trans. 2 **1979**, 342 (1979).
[13]M. J. Kamlet and R. W. Taft, J. Chem. Soc., Perkin Trans. 2 **1979**, 337 (1979).
[14]M. Pecul and K. Ruud, Adv. Quantum Chem. **50**, 185 (2005).
[15]T. Crawford, Theor. Chem. Acc. **115**, 227 (2006).
[16]T. D. Crawford, M. C. Tam, and M. L. Abrams, J. Phys. Chem. A **111**, 12057 (2007).
[17]P. L. Polavarapu, Chem. Rec. **7**, 125 (2007).
[18]T. D. Crawford and P. J. Stephens, J. Phys. Chem. A **112**, 1339 (2008).
[19]J. Autschbach, Chirality **21**, E116 (2009).
[20]T. B. Pedersen, J. Kongsted, and T. D. Crawford, Chirality **21**, S68 (2009).
[21]K. Ruud, P. J. Stephens, F. J. Devlin, P. R. Taylor, J. R. Cheeseman, and M. J. Frisch, Chem. Phys. Lett. **373**, 606 (2003).
[22]M. C. Tam, N. J. Russ, and T. D. Crawford, J. Chem. Phys. **121**, 3550 (2004).
[23]J. Kongsted, T. B. Pedersen, M. Strange, A. Osted, A. E. Hansen, K. V. Mikkelsen, F. Pawlowski, P. Jorgensen, and C. Hättig, Chem. Phys. Lett. **401**, 385 (2005).
[24]K. Ruud and R. Zanasi, Angew. Chem., Int. Ed. Engl. **44**, 3594 (2005).
[25]J. Kongsted, T. B. Pedersen, L. Jensen, A. E. Hansen, and K. V. Mikkelsen, J. Am. Chem. Soc. **128**, 976 (2006).
[26]T. D. Crawford, M. C. Tam, and M. L. Abrams, Mol. Phys. **105**, 2607 (2007).
[27]T. B. Pedersen, J. Kongsted, T. D. Crawford, and K. Ruud, J. Chem. Phys. **130**, 034310 (2009).
[28]T. Muller, K. B. Wiberg, and P. Vaccaro, J. Phys. Chem. A. **104**, 5959 (2000).
[29]S. M. Wilson, K. B. Wiberg, J. R. Cheeseman, M. J. Frisch, and P. H. Vaccaro, J. Phys. Chem. A **109**, 11752 (2005).
[30]K. B. Wiberg, P. H. Vaccaro, and J. R. Cheeseman, J. Am. Chem. Soc. **125**, 1888 (2003).
[31]K. B. Wiberg, Y.-G. Wang, P. H. Vaccaro, J. R. Cheeseman, and M. R. Luderer, J. Phys. Chem. A **109**, 3405 (2005).
[32]M. C. Tam, M. L. Abrams, and T. D. Crawford, J. Phys. Chem. A **111**, 11232 (2007).
[33]T. D. Crawford and W. D. Allen, Mol. Phys. **107**, 1041 (2009).
[34]J. G. Kirkwood, J. Chem. Phys. **2**, 351 (1934).
[35]M. Born, Z. Phys. A: Hadrons Nucl. **1**, 45 (1920).
[36]L. Onsager, J. Am. Chem. Soc. **58**, 1486 (1936).
[37]J. Tomasi, Theor. Chem. Acc. **112**, 184 (2004).
[38]B. Mennucci, J. Tomasi, R. Cammi, J. R. Cheeseman, M. J. Frisch, F. J. Devlin, S. Gabriel, and P. J. Stephens, J. Phys. Chem. A **106**, 6102 (2002).
[39]M. Pecul, D. Marchesan, K. Ruud, and S. Coriani, J. Chem. Phys. **122**, 024106 (2005).
[40]P. J. Stephens, F. J. Devlin, C. F. Chabalowski, and M. J. Frisch, J. Phys. Chem. **98**, 11623 (1994).
[41]A. D. Becke, J. Chem. Phys. **98**, 5648 (1993).
[42]C. Lee, W. Yang, and R. G. Parr, Phys. Rev. B. **37**, 785 (1988).
[43]L. A. Curtiss and K. Raghavachari, Theor. Chem. Acc. **108**, 61 (2002).
[44]M. J. Frisch, G. W. Trucks, H. B. Schlegel *et al.*, GAUSSIAN 03, Revision C.02, Gaussian, Inc., Wallingford, CT, 2004.
[45]T. D. Crawford and H. F. Schaefer, in *Reviews in Computational Chemistry*, edited by K. B. Lipkowitz and D. B. Boyd (VCH, New York, 2000), Vol. 14, Chap. 2, pp. 33–136.
[46]I. Shavitt and R. J. Bartlett, *Many-Body Methods in Chemistry and Physics: MBPT and Coupled-Cluster Theory* (Cambridge University Press, Cambridge, 2009).
[47]H. Koch and P. Jørgensen, J. Chem. Phys. **93**, 3333 (1990).
[48]O. Christiansen, H. Koch, and P. Jørgensen, Chem. Phys. Lett. **243**, 409 (1995).
[49]M. E. Casida, *Recent Advances in Density Functional Methods* (World Scientific, Singapore, 1995).
[50]J. R. Cheeseman, M. J. Frisch, F. J. Devlin, and P. J. Stephens, J. Phys. Chem. A **104**, 1039 (2000).
[51]F. London, J. Phys. Radium **8**, 397 (1937).
[52]R. Ditchfield, Mol. Phys. **27**, 789 (1974).
[53]T. B. Pedersen, H. Koch, L. Boman, and A. M. J. S. de Meras, Chem. Phys. Lett. **393**, 319 (2004).
[54]T. H. Dunning, J. Chem. Phys. **90**, 1007 (1989).
[55]D. E. Woon and T. H. Dunning, J. Chem. Phys. **100**, 2975 (1994).
[56]C. J. Harding and I. Powis, J. Chem. Phys. **125**, 234306 (2006).
[57]D. A. McQuarrie, *Statistical Thermodynamics* (University Science Books, Mill Valley, California, 1973).
[58]W. J. Hehre, L. Radom, P. v.R. Schleyer, and J. A. Pople, *Ab Initio Molecular Orbital Theory* (Wiley, New York, 1986).
[59]M. J. Frisch, G. W. Trucks, H. B. Schlegel *et al.*, GAUSSIAN 09, Revision A.1, Gaussian, Inc.

[60]T. D. Crawford, C. D. Sherrill, E. F. Valeev, J. T. Fermann, R. A. King, M. L. Leininger, S. T. Brown, C. L. Janssen, E. T. Seidl, J. P. Kenny, and W. D. Allen, J. Comput. Chem. **28**, 1610 (2007).
[61]L. A. Curtiss, P. C. Redfern, K. Raghavachari, V. Rassolov, and J. A. Pople, J. Chem. Phys. **110**, 4703 (1999).
[62]H. Landolt, *The Optical Rotating Power of Organic Substances and its Applications* (Chemical Publishing Co., 1902).
[63]E. Eliel, S. Wilen, and M. Doyle, *Basic Organic Stereochemistry* (Wiley-Interscience, 2001).
[64]P. L. Polavarapu, A. Petrovic, and F. Wang, Chirality **15**, S143 (2003).
[65]See supplementary material at http://dx.doi.org/10.1063/1.3693270 for all the Drude model fit parameters and the calculated rotational strengths.
[66]H. G. Rule and A. McLean, J. Chem. Soc. **1932**, 1400 (1932).
[67]H. G. Rule and J. P. Cunningham, J. Chem. Soc. **1935**, 1038 (1935).
[68]Y. Kumata, J. Furukawa, and T. Fueno, Bull. Chem. Soc. Jpn. **43**, 3663 (1970).
[69]K. B. Wiberg, Y. gui Wang, S. M. Wilson, P. H. Vaccaro, and J. R. Cheeseman, J. Phys. Chem. A **105**, 3448 (2005).
[70]N. Hammer, K. Diri, K. D. Jordan, C. Desfrançois, and R. N. Compton, J. Chem. Phys. **119**, 3650 (2003).
[71]C. Desfrançois, H. Abdoul-Carime, and J.-P. Schermann, Int. J. Mod. Phys. B **10**, 1339 (1996).
[72]R. C. Fortenberry and T. D. Crawford, J. Chem. Phys. **134**, 154304 (2011).
[73]R. C. Fortenberry and T. D. Crawford, J. Phys. Chem. A **115**, 8119 (2011).
[74]J. Simons, Ann. Rev. Phys. Chem. **62**, 107 (2011).
[75]T. Klahn and P. Krebs, J. Chem. Phys. **109**, 543 (1998).
[76]P. Mikulski, T. Klahn, and P. Krebs, Phys. Rev. A **55**, 369 (1997).
[77]S. Ard, W. Garrett, R. Compton, L. Adamowicz, and S. Stepanian, Chem. Phys. Lett. **473**, 223 (2009).
[78]J. Neugebauer, E. J. Baerends, M. Nooijen, and J. Autschbach, J. Chem. Phys. **122**, 234 (2005).
[79]M. Nooijen, Int. J. Quantum Chem. **106**, 2489 (2006).
[80]L. D. Bari and G. Pescitelli, *Computational Spectroscopy Methods, Experiments and Applications* (Wiley), pp. 241–277.